

An Investigation of Search Algorithms for Aerial Reconnaissance of an Area Target

Rory Blankenship¹, James Bluman¹, and Josiah Steckenrider²

¹Department of Mathematical Sciences
United States Military Academy
West Point, NY 10996

²Department of Civil and Mechanical Engineering
United States Military Academy
West Point, NY 10996

Corresponding author's Email: john.steckenrider@westpoint.edu

Abstract: As drone technology becomes increasingly accessible in commercial and defense sectors, it is important to establish efficient ways of employing the technology to leverage its inherent advantages. In the context of a chemical, biological, radiological, and nuclear (CBRN) attack, an unmanned aerial system (UAS) can provide an understanding of the area affected by contaminants in a faster and safer way than a manned reconnaissance mission. Commonly used deterministic paths provide comprehensive coverage but they can require a substantial amount of time to reach each sector within a search space. The recently proposed Lissajous search pattern provides easily tunable parameters that can be adjusted according to the search space and anticipated size of the target. This paper provides an evaluation of Lissajous patterns against canonical search patterns and investigates ways of maximizing their efficiency for various target sizes.

Keywords: Lissajous curves, Drones, Unmanned Aerial System, Optimal Search Patterns

1. Introduction

The success of search operations is contingent on how quickly targets can be located where the likelihood of survival diminishes rapidly, or the danger can spread quickly with time. Chemical, Biological, Radiological, and Nuclear (CBRN) attacks become more deadly as they diffuse from the point of attack. Human-led teams risk exposure to the contaminants and are limited by their ability to traverse the search space quickly and effectively. Unmanned aerial systems (UAS) require less manpower and are able to operate better, particularly in areas with obstructed terrain, given their ability to pass over obstacles, negotiate changes in elevation, and provide better range (Kopeikin et al., 2019; Munera, 2019). With continuous advances and rising interest in drone technology, UASs have become the preferred method of search (Araujo, Valente, Kooistra, Munniks, & Peters, 2020). As the faster, safer, less costly alternative, UAS based reconnaissance will continue to replace human search parties creating a need for optimal flight paths. In this paper we suggest alternative forms of widespread, well-known patterns and compare the effectiveness of each. Further, we will introduce a new method of search generation using the Lissajous curve which does not display the same shortcomings of the other patterns.

1.1 Related Work

Similar research focuses on one of two areas for developing search patterns. The first area focuses on either improving deterministic solutions to make them more efficient. The second approach focuses uses more intelligent cycles which require informed updates to continually generate waypoints. Information-theoretic approaches require a feedback loop that require UASs to identify ground conditions in order to methodically calculate subsequent waypoints. Echeveste, Lee, and Clark (2021) create a search pattern that is updated one point at a time using Kriging variance and new information ascertained in previous iterations. To begin, the UAS samples five randomly selected points to map the variance within the area of interest. Through each iteration the next waypoint is determined using variance driven sampling which identifies the point with the highest variance. This method establishes a fair understanding of the search space within a small number of points by checking locations where the most uncertainty exists, but the locations are chosen without consideration to the distance between points creating unnecessarily long paths. Using a similar framework, Rahmes, Chester, Hunt, and Chiasson (2018) use game theory to create probabilistic predictions of the target location. Points are selected according to the probability of finding the target at that point. After each iteration, the probabilistic map is updated, and the next point is chosen. Martins and Gustavo (1993) suggest using

branch-and-bound algorithm informed by the probability the target exists within each sector to consider an exhaustive set of possible solutions. The UAS then moves to the adjacent sector with the greatest probability of finding the target and recalculates the probability of success for all existing solutions. Different methods of branch-and-bound are applied with different search spaces in order to determine which method is most successful at varying distances.

Research proposed by San Juan, Santos, and Andujar, (2018) suggest different methods of dividing the space into cells and weighting each based on the probability the target exists within that cell and the distance it is from the current cell. The result is a deterministic path that veers back and forth across the search space inefficiently chasing cells with the highest probability and creating an unnecessarily long search. Additionally, this method requires a considerable amount of initial information about the likelihood of a target's location. Other research suggests fitting a pattern to a unique existing search space rather than limiting the area to a perfect square, but ultimately relies on the most simplistic canonical pattern (Wollan, 2004). Commonly used deterministic patterns are given by the International Aeronautical and Maritime Search and Rescue Manual (IAMSAR) (IAMSAR, 2016). Figure 1 shows the existing patterns as well as an example of a possible Lissajous curve.

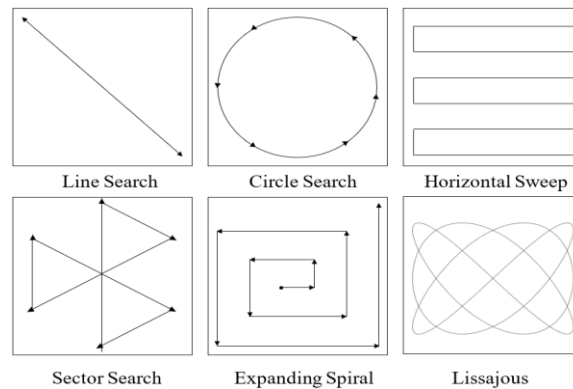


Figure 1. Existing Deterministic Search Paths

Search paths can be designed to intercept a moving target hence electing for a cyclical design in which the search agent retraces its path or methodically searches the entire area to locate a static target. Steckenrider, Leamy, and Furukawa (2020) suggests a hybrid pattern that doubles back on itself creating intersections while continuously searching new regions within the search space. Using the Lissajous curve to create a deterministic flight path has the potential to offer advantages over the canonical patterns (Steckenrider, 2021). This research will focus on generating a Lissajous pattern tailored to the search space and specifications of the target. In order to mimic the behavior of a CBRN agent the target will cover a fixed area, and the UAS will search until it successfully detects the contaminant. The most appropriate Lissajous patterns will be compared to the canonical patterns as well as proposed variants to the canonical patterns to determine which search path is most efficient.

1.2 Chemical Detection

CBRN attacks occur in two stages that control how the agent is spread: delivery and dissemination. Delivery is the method used to release the contaminant, the most common of which uses an explosive charge that disperses the chemicals laterally (Kimball & Davenport, 2020). The method of delivery effects the concentration of particles and the total area affected by the attack. CBRN attacks delivered by artillery rounds or ground detonated systems release the contaminant at the point of impact resulting in smaller, concentrated clouds. Methods that disperse the attack in flight such as airbursts from ballistic missiles, cruise missiles, or UAVs result in a less concentrated plume over a larger area. Particles spread according to the method of delivery used for approximately 30 seconds before atmospheric conditions and terrain begin to exert a larger influence (US Army Field Manual, 1986). Both atmospheric stability and wind speed have significant effects on the downwind distance an agent will travel and its concentration over time. Dispersion categories exist on a scale ranging from 1, very unstable, to 7, extremely stable, and can be used to assess how airborne particles will travel. The dispersion category is determined by atmospheric stability which can be roughly gauged by wind speed, the time of day, whether the attack occurred near a coastal site, and the cloud coverage as given in meteorological reports. Conditions contributing to increased instability include colder temperatures, increased cloud coverage, and higher wind speeds. In stable conditions chemical cloud width remains nearly constant. For the purpose of this research the conditions are assumed to be such that the target behavior and static and the area affected is constant throughout the search.

2. Generation of Deterministic Search Patterns

Deterministic search patterns calculate every waypoint charting the entire path before the UAS begins its search. One of the advantages this method offers is eliminating the need for a sustained connection to remote systems for path updates which may extend the operable range of the search agents. Furthermore, the paths require that minimal information be inferred about the target and search space, and unlike the information-theoretic approaches, they are created such that points are searched in the shortest possible course. The general formulas for generating all six paths are outlined below. Each search pattern begins at the point (1,0) to standardize starting positions and emulate realistic field conditions where a UAS would be employed from a point along the perimeter. For each pattern we will test the standard design as well as a similar alternative intended to be more efficient and compare all six results. The resulting patterns created for a target covering 4% of the total search area are shown in Figure 2, where standard patterns are shown in black and modified patterns in orange.

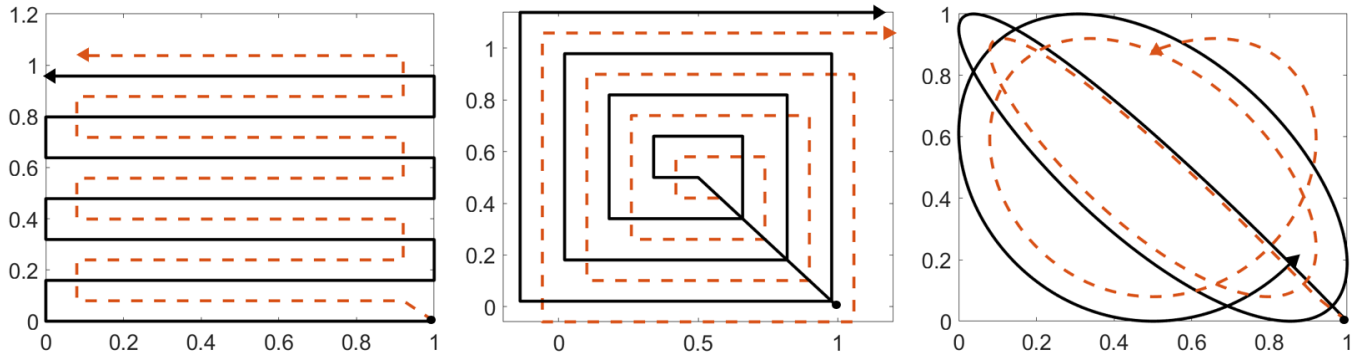


Figure 2. Standard and Modified Deterministic Search Paths for 4% Area Target

2.1 Horizontal Sweep

The first and most common canonical search pattern is the horizontal sweep (HS), given by Equation 1. The horizontal sweep searches the width of the field at regular vertical intervals determined by the size of the target. The optimal change in height between horizontal sweeps is given by $\Delta H = 2R/\sqrt{2}$ where the vertical shift is as large as possible without missing targets located between the passes. The alternative horizontal sweep follows the same motion but establishes a space of $R/\sqrt{2}$ space between the search path and boundaries. This ensures targets within the 1×1 domain will be detected without incidentally searching outside the feasible target region.

$$\begin{bmatrix} x_k \\ y_k \\ \theta_k \end{bmatrix} = \begin{bmatrix} x_{k-1} \\ y_{k-1} \\ \theta_{k-1} \end{bmatrix} + \begin{bmatrix} D_{k-1} \sin \theta_{k-1} \\ D_{k-1} \cos \theta_{k-1} \\ \frac{\pi}{2} \sqrt{2} \sin\left(\frac{\pi(k-1)}{2} - \frac{\pi}{4}\right) \end{bmatrix} \quad (1)$$

where

$$D_{k-1} = \begin{cases} \Delta H, & k-1 \text{ is even} \\ W, & k-1 \text{ is odd} \end{cases} \quad (2)$$

The width of the search region, W , and the vertical space between sweeps, ΔH , can be adjusted to generate either the standard horizontal sweep or the modified horizontal sweep.

2.2 Expanding Spiral

The expanding spiral (ES) moves initially in the direction of the center of the search domain and then begins searching outward in incrementally larger squares. The standard expanding spiral travels to the point (0.5, 0.5) and then begins the search

pattern whereas the alternative expanding spiral travels to the point $(0.5 - \sqrt{2}, 0.5 - \sqrt{2})$ in order to center the entire search around the point $(0.5, 0.5)$. The waypoints for both variants are given by Equation 3:

$$\begin{bmatrix} x_k \\ y_k \\ \theta_k \end{bmatrix} = \begin{bmatrix} x_k - 1 \\ y_k - 1 \\ \theta_k - 1 \end{bmatrix} + \begin{bmatrix} D_{k-1} \cos \theta_{k-1} \\ D_{k-1} \sin \theta_{k-1} \\ \frac{\pi}{2} \end{bmatrix} \quad (3)$$

where

$$D_{k-1} = D[(k - 1)/2] \quad (4)$$

and D is a distance parameter governed by the size of the search space.

2.3 Lissajous Search Patterns

Lissajous search patterns are parametric curves displaying simple harmonic motion in the x and y direction. The modified Lissajous pattern (LP) is created using the same parameters but similarly to the horizontal sweep the modified LP does not search to the edges of the search domain, rather it maintains the same distance of $R/\sqrt{2}$ from the boundaries. The waypoints for the LP can be generated as follows:

$$\begin{bmatrix} x_k \\ y_k \end{bmatrix} = \begin{bmatrix} X \sin(\omega_x k \Delta t + \varphi_x) + \bar{x} \\ Y \sin(\omega_y k \Delta t + \varphi_y) + \bar{y} \end{bmatrix} \quad (5)$$

where X and Y are half the x and y dimensions of the rectangular bounds of the curve and can be adjusted to generate a modified LP with tighter edges. The angular frequencies, $\omega_{x,y}$, determine the shape of the LP, $\varphi_{x,y}$ is the phase shift, and $[\bar{x} \ \bar{y}]^T$ fixes the center of the pattern. Variations in the frequency ratio of ω_x to ω_y (Eq. 6) from 0 to 1 yield an infinitely diverse number of patterns, where irrational frequency ratios create nonrecurring patterns.

$$r_\omega = \frac{\omega_x}{\omega_y} \quad (6)$$

Figure 3 gives several examples of Lissajous curves that can be created by altering the frequency ratio and phase shift.

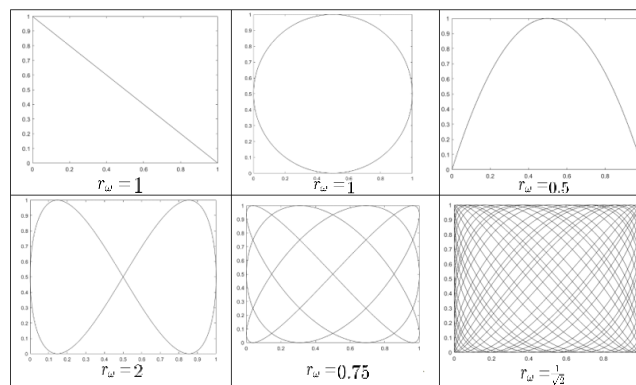


Figure 3. Lissajous Patterns with Varying Frequency Ratios r_ω

3. Evaluation of The Lissajous Pattern

The expanding spiral and horizontal sweep are optimized by maximizing the possible space between iterations. This ensures the most efficient version of each pattern is generated while eliminating the possibility of missing a target in the interspace. In order to determine the best frequency ratio for the LP at different target sizes, 1000 irrational frequency ratios

from 0 to 1 were tested in increments of $\gamma = \frac{0.0014}{\sqrt{2}}$. Each frequency ratio was used in 10,000 Monte Carlo simulations where the time k it took to find the target was determined. The best frequency ratio was selected from those tested and used to compare relative success between all patterns.

3.1 Success Measures

Patterns were originally evaluated at a single threshold that offered an adequate level of confidence while restricting the amount time allowed to search such as the 80th or 90th percentile. Due to the flexibility of the LP, a frequency ratio can be found that minimizes the amount of time to reach the designated threshold, however these patterns perform worse than the canonical patterns at nearly all other points along the cumulative distribution function (CDF). Its ability to edge out the other patterns at a single point suggests it may be the preferred pattern for clearing an area given a specific amount of time to search. However, to determine the best overall pattern, a more comprehensive evaluation of the CDFs is required. Stochastic dominance is an axiom of utility theory that provides an arithmetical metric for preference orderings (Quirk, James, & Saposnik, 1962). Stochastic dominance can be established by evaluating the area under the curve (AUC) for each pattern up to the designated thresholds. First-order stochastic dominance occurs when one CDF performs better than all the others for every point along the graph. Second-order stochastic dominance determines which CDF is the best overall. Equation 7 gives the formula for second-order stochastic dominance from time 0 to the percentile threshold, T where one random process R dominates the other, R' (Fishburn, 1980):

$$\int_0^T F_R(t)dt > \int_0^T F_{R'}(t)dt \quad \forall t \in \mathbb{R} \quad (7)$$

Rather than determining the pattern that performs best at a single arbitrary percentile, Equation 7 evaluates the search paths in full up to the thresholds. The 80th percentile was selected as a boundary for measuring the AUC to capture which pattern does best within a limited amount of time. Regardless of target size the HS always finishes a complete sweep of the domain first but is outperformed by other patterns for a majority of the search. Given circumstances in which there is not enough time for an exhaustive search it is advantageous to employ a method that locates the most targets in earlier stages.

4. Results

4.1 CDF Shapes

The shapes of each CDF are indicative of the patterns' strengths and weaknesses as well as their unique behavior. Figure 4 shows the CDFs for all six patterns evaluated at the 80th percentile of the standard horizontal sweep for targets covering 1, 4, and 12% of the entire search space.

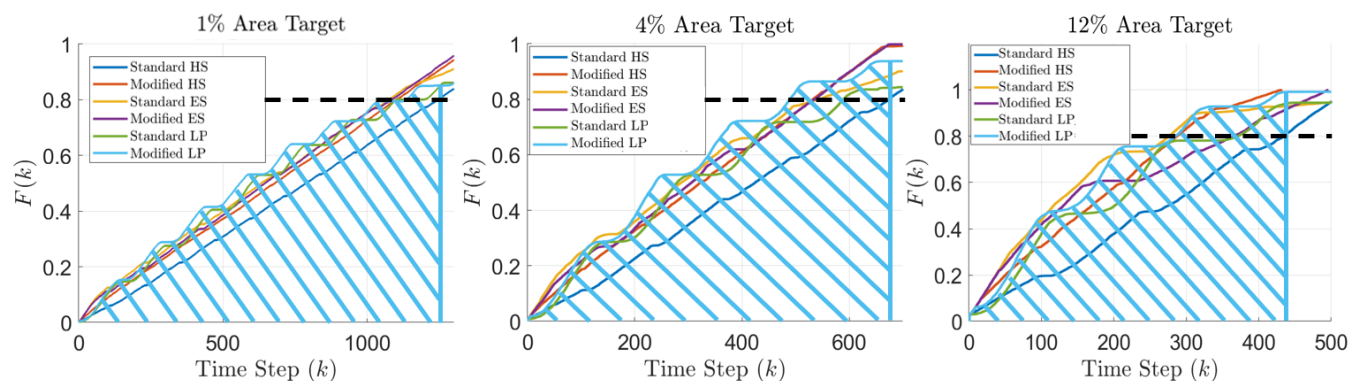


Figure 4. CDF Results for Varying Target Sizes

The standard HS follows a roughly linear trend consistently performing worst across target sizes. This pattern is slightly less efficient during the first sweep because it searches along the bottom edge of the domain incorporating some infeasible target areas. The small elbows in the curve are created by the vertical sweeps between passes. The modified HS produces a similar CDF, however the first sweep is more efficient because the search is entirely contained to the feasible target

region. The elbows in the modified HS are also smaller because the UAS only travels as far as necessary to detect any possible targets. The final sweep is less efficient as the UAS makes one final pass including some area above the search space; this is shown by the leveling of the CDF as the HS approaches completion. The modified HS always reaches finds 100% of the targets and is therefore the best pattern for an exhaustive search.

The expanding spiral begins its outward search from the center of the domain alternating between horizontal and vertical sweeps that increase by $2r/\sqrt{2}$ each round. Elbows in the ES are a result of the points where the pattern crosses over the original diagonal trace from the point (1,0). The modified ES begins searching in a spiral shape at the point $(0.5 - \sqrt{2}, 0.5 - \sqrt{2})$ consequently overlapping itself before the standard expanding spiral and creating earlier elbows in the curve. The CDF slopes are very similar for both patterns until the final elbow where the modified expanding spiral performs slightly better due to being centered around the point (0.5, 0.5).

The Lissajous pattern has elbows in the curve for instance the pattern intersects itself. Because the modified LP does not search to the edges of the domain the turns are made sooner shifting the modified LP CDF to the left. Moreover, traveling within closer boundaries allows the modified LP to complete more of the search pattern in the same number of time steps. For smaller target sizes, the modified LP has an additional elbow because it is able to make another turn within the same number of steps.

4.2 Area Under the Curve

The AUC indicates which patterns perform best up to the 80th percentile. Table 1 shows the AUCs for all six patterns, at both percentile thresholds and at five different target area percentages.

Table 1. AUC Results for Varying Target Sizes at the 80th Percentile

	Standard			Modified		
	HS	ES	LP	HS	ES	LP
1%	496	593	600 (949γ)	581	594	630 (939γ)
2%	358	452	441 (918 γ)	443	458	480 (920γ)
4%	265	363	338 (872 γ)	352	366	381(884γ)
8%	193	280	259 (857 γ)	279	297	304 (865γ)
12%	180	283	257 (822 γ)	262	248	277 (830γ)

Among the standard patterns the ES performed best for nearly all target sizes while the HS was the worst overall method of search. For the target covering 1% of the overall search area the LP outperformed the ES by only 1.2%. However, as the target size increases the standard ES becomes the better overall pattern outperforming the LP by over 10%. The modified LP is the best overall search pattern with the largest AUC for nearly all target sizes. The same decrease in relative fitness occurs for the modified LP which outperformed the modified ES by 6.1% for the smallest but had a smaller AUC than the standard ES for the largest target. The modified HS and LP were significantly more efficient for all target sizes than the standard counterparts while both variants of the expanding spiral performed similarly.

5. Conclusions and Future Work

Results from this research indicate that the best search algorithm is contingent upon the anticipated size of the target and the amount of time available for search. Given an unlimited amount of time to do a comprehensive search of the domain the modified horizontal sweep performs a complete search in the least amount of time. The Lissajous curve by comparison is the worst method for comprehensive area coverage. For smaller targets the LP is the preferred method while targets expected to cover more than approximately 8% of the search space should defer to the expanding spiral. As the target size increases, the best frequency ratio r_ω decreases from 0.94-0.81 for the standard pattern and 0.93-0.82 for the modified pattern. As the frequency ratio decreases, the pattern becomes looser leaving larger gaps between loops to adjust to larger target sizes. The tendency to fit a pattern that maximizes the space between iterations while reducing the probability of missing a target is congruent with the rationale for spacing within the canonical patterns.

One of the current assumptions for this model is perfect detection when the drone flies within the radius of the target. Future work should focus on incorporating the principles of particle concentration where the CBRN agent is most potent at the point of attack and dissipates as it moves away from the source. The probability of detecting the target directly above the focal point of the attack would be the highest and diminish moving outward.

6. References

- Araujo, J. O., Valente, J., Kooistra, L., Munniks, S., & Peters, R. J. (2020). Experimental flight patterns evaluation for a UAV-based air pollutant sensor. *Micromachines*, 11(8), 768.
- Army, U. S. (1986). FM 3-6 AMF 105-7 FM 7-11-H. Field Behavior of NBC Agents (Including Smoke and Incendiaries).
- Echeveste, D., Lee, A., & Clark, N. (2021). Using Spatial Uncertainty to Dynamically Determine UAS Flight Paths. *Journal of Intelligent & Robotic Systems*, 101(4), 1-16.
- Fishburn, P. C. (1980). Stochastic dominance and moments of distributions. *Mathematics of operations Research*, 5(1), 94-100.
- IMO. (2016). IAMSAR Manual: International Aeronautical and Maritime Search and Rescue Manual.
- Kimball, D., & Davenport, K. (2018). Chemical Weapons: Frequently Asked Question. *Arms Control Association*.
- Kopeikin, A., Heider, S., Larkin, D., Korpela, C., Morales, R., & Bluman, J. E. (2019). Unmanned aircraft system swarm for radiological and imagery data collection. In *AIAA Scitech 2019 Forum*
- Martins, G. H. (1993). *A new branch-and-bound procedure for computing optimal search paths*. Naval Postgraduate School, Monterey CA.
- Munera, A. (2019). Chemical, Biological, Radiological, and Nuclear Operations, *US Army Field Manual 3-11*, Washington, D.C.
- Quirk, J. P., & Saposnik, R. (1962). Admissibility and measurable utility functions. *The Review of Economic Studies*, 29(2), 140-146.
- Rahmes, M., Chester, D., Hunt, J., & Chiasson, B. (2018, May). Optimizing cooperative cognitive search and rescue UAVs. In *Autonomous Systems: Sensors, Vehicles, Security, and the Internet of Everything* (Vol. 10643, p. 106430T). International Society for Optics and Photonics.
- San Juan, V., Santos, M., & Andújar, J. M. (2018). Intelligent UAV map generation and discrete path planning for search and rescue operations. *Complexity*, 2018.
- Steckenrider, J. J. (2021). Adaptive Aerial Localization Using Lissajous Search Patterns. *IEEE Transactions on Robotics*.
- Steckenrider, J. J., Leamy, S., & Furukawa, T. (2020, November). Cooperative Aerial Search and Localization Using Lissajous Patterns. In *2020 IEEE International Symposium on Safety, Security, and Rescue Robotics (SSRR)* (pp. 233-240). IEEE.
- Wollan, H. (2004). Incorporating heuristically generated search patterns in search and rescue. *University of Edinburgh*.